Petroleum Science 19 (2022) 2995–3003

Contents lists available at ScienceDirect

Petroleum Science

journal homepage: www.keaipublishing.com/en/journals/petroleum-science

Original Paper

Multi-objective optimization design of deviation-correction trajectory considering the production loss in shale gas cluster well

Zi-Jun Dou [a], Yong-Sheng Liu [a, *], Xing Qin [b], De-Li Gao [c], Gan-Sheng Yang [a]

[a] Key Laboratory of Deep Geological Drilling Technology of Ministry of Natural Resources, China University of Geosciences, Beijing 100083, China
[b] Sinopec Research Institute of Petroleum Engineering, Beijing 100101, China
[c] MOE Key Lab of Petroleum Engineering, China University of Petroleum, Beijing 102249, China

ARTICLE INFO

Article history:
Received 30 May 2022
Received in revised form
24 July 2022
Accepted 22 September 2022
Available online 27 September 2022
Handling Editor: Zhi-Ming Chen
Edited by Jia-Jia Fei

Keywords:
Shale gas
Inter-fracture interference effect
Production loss
Deviation-correction trajectory
Multi-objective optimization

ABSTRACT

In shale gas mining, the inter-fracture interference effect will significantly occur if the actual well deviates from the planned trajectory. To reduce production loss, operators want to get back on the planned trajectory economically and safely. Based on this, a multi-objective optimization model of deviation-correction trajectory is established considering the production loss evaluation. Firstly, the functional relationship between the production envelope and the fracturing depth is constructed, and the production loss is obtained by combining the calculation method of volume flow. Based on the proposed "double-arc" trajectory design method, the production loss of the fracture on the deviation-correction trajectory is obtained. Finally, combined with the well profile energy evaluation, a new optimization model of deviation-correction trajectory is established. The results demonstrate that after optimizing the fracturing depth, the production loss of the deviation-correction trajectory is reduced by 13.2%. The maximum curvature value results in a trajectory with a minimum production loss yet a maximum well profile energy. The proposed model reduces the well profile energy by 15.6% compared with the existing model. It is proved that the proposed model can reduce the probability of drilling accidents and achieve high gas production in the later mining stage. This study fully considers various factors affecting horizontal wells in the fracturing area, which can provide theoretical guidance for the design of deviation-correction trajectory.

1. Introduction

Shale gas reservoir is characterized by poor quality and difficult exploitation (Shandrygin, 2019), and it is difficult to obtain good results by conventional exploitation methods (Dou et al., 2022). Currently, horizontal drilling and hydraulic fracturing are hot stimulation methods for shale gas reservoirs (Bagherian et al., 2010). During horizontal drilling in a fracturing area, if the actual well deviates from the planned trajectory, the inter-fracture interference will significantly occur (Maus and DeVerse, 2016). In order to reduce production loss, it is necessary to optimize the design of the deviation-correction trajectory. Liu et al. firstly proposed a trajectory design method in which the direction of the target trajectory is constrained (Liu and Shi, 2002). After that, Lee et al. presented a method to design trajectory using genetic algorithm, which took drilling locations and costs into account (Lee et al., 2009). Liu et al. came up with a deviation-correction trajectory control model on account of the minimum well profile energy criterion (Liu and Samuel, 2016). Wang et al. presented a mathematical design formula for modified trajectory in the case of uncertain target points comprehensively considered well profile energy and trajectory length (Wang and Gao, 2016). A method to optimize the target and trajectory in the context of geological uncertainty was put forward by Hanea et al. (2017). Lyu et al. proposed a model for automatic identification of trajectory in fracturing area on the basis of the rapid propulsion method (Lyu et al., 2021). However, a literature review reveals that the production loss has not been considered in previous studies. The existing models cannot obtain optimal deviation-correction effect in the fracturing area.

Regarding production loss prediction, Giger firstly used mathematical models to analyze the production of fractured horizontal wells (Giger, 1984). Conlin et al. established a production prediction model with simplified fracture morphology based on Giger model

* Corresponding author.
E-mail address: yongsheng@cugb.edu.cn (Y.-S. Liu).

https://doi.org/10.1016/j.petsci.2022.09.024

(Conlin et al., 1990). Soliman et al. considered the inter-fracture interference effect and studied the relationship between fracture parameters and production (Soliman et al., 1996). Yao et al. applied the elliptical flow concept to predict the adjacent fractures' production (Yao et al., 2013). The existing models can predict production loss in vertical well but not the deviation-correction trajectory. Based on this, the inter-fracture interference effect on the deviation-correction trajectory is studied.

2. Inter-fracture interference effect

2.1. Production envelope

In order to extract shale gas, hydraulic fracturing is used to break up rock and create artificial fractures. Shale gas flows from the formation into the fracture, forming a production envelope around the well (Fisher et al., 2005). Due to the limited volume covered by the envelope, it is necessary to drill multiple horizontal wells to realize the full potential of the reservoir. Horizontal wells are drilled at the planning spacing, and the well spacing shall ensure that the production envelope contact but does not overlap.

However, because of measurement accuracy limitations, drilling errors often result in a deviation of several hundred feet from the planned fracture location. If the deviation is not corrected in time, the production envelope among wells may cross and overlap. On the one hand, wells too far apart to completely empty the reservoir can leave the untapped area in the formation. On the other hand, close wells compete for overlap area at the junction, which significantly impacts production (Fig. 1).

The production envelope does not come from a fixed volume around the well which should consider fracture propagation, rock characteristics, and formation-specific fluid properties (Ozkan et al., 2011). Because of the distribution of fractures near the well, the pressure drop funnel is elliptical instead of circular (Lu et al., 2009). Assuming that all production occurs in a particular formation, the seepage pressure disturbance defines the production envelope. The long and short axis of production envelope is mainly controlled by production time (Magalhaes et al., 2007). As shown in Fig. 2, the long and short axis of the ellipsoid gradually increased with time (Yao et al., 2013).

The volume of the control ellipsoid is calculated as follows:

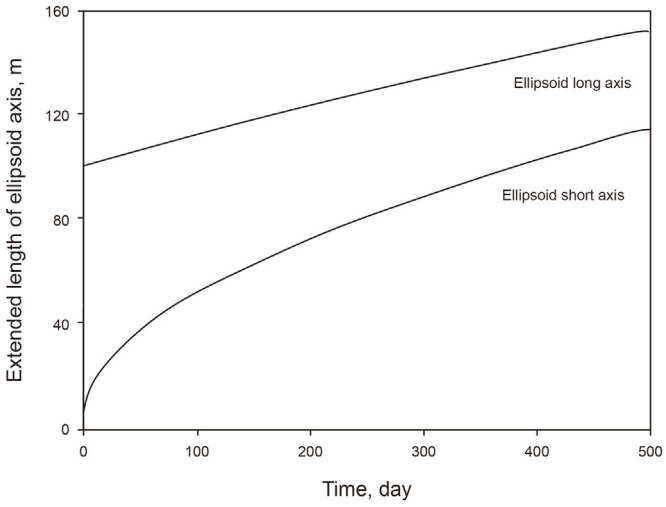

Fig. 2. Diagram of control ellipsoid radius over time.

$$V = \frac{4\pi a \cdot b^2}{3} \tag{1}$$

$$a = x_f \cdot \mathrm{ch}\xi_R \tag{2}$$

$$b = x_f \cdot \mathrm{sh}\xi_R \tag{3}$$

where,

$$\xi_R = 0.5 \ln\left[12t_D + 1 + \sqrt{(12t_D + 1)^2 - 1}\right] \tag{4}$$

$$t_D = \frac{k_f t}{\mu\varphi c x_f^2} \tag{5}$$

ξ_R is the outer boundary of the ellipsoid; x_f is the fracture length; t_D is dimensionless time; k_f is fracture permeability; t is production time; μ is natural gas viscosity; φ is porosity; c is the comprehensive compressibility coefficient of gas reservoir.

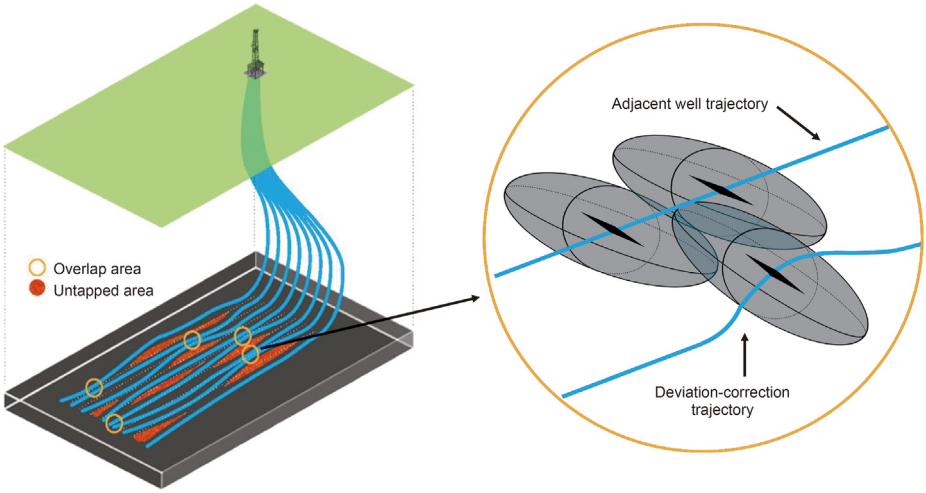

Fig. 1. Schematic diagram of inter-fracture interference effect.

2.2. Production loss

Based on the above, the inter-fracture interference will appear when the gas reservoir is exploited for a certain period. To calculate the production loss, the production of a single fracture is first analyzed.

Due to the existence of fracture, the conductivity of fracture near-horizontal well is powerful (Lei et al., 2007). Once the gas in the matrix flows into the fracture, its seepage velocity increases rapidly. When the seepage velocity is large, it will enter the thoroughly turbulent section. At this time, the pressure gradient is directly proportional to the square of the seepage velocity. The equation describing the high-speed non-Darcy seepage in the fracture is:

$$\frac{\mathrm{d}p}{\mathrm{d}x}=\frac{\mu}{k}v+\beta\rho_g v^2 \tag{6}$$

where, v is the seepage velocity of natural gas; ρ_g is the natural gas density under the condition of gas reservoir; $\beta = 0.005/(\varphi^{5.5}/k^{5.5})$; k is the permeability of gas reservoir.

The seepage velocity in the fracture can be expressed as:

$$v=\frac{\rho_{sc}q}{\rho_g w_f h} \tag{7}$$

where, ρ_{sc} is the density of natural gas under standard conditions; w_f is the fracture width; q is the gas production under standard conditions; h is the effective thickness of gas reservoir.

The density of natural gas under standard conditions is:

$$\rho_{sc}=\frac{p_{sc}M}{R_g T_{sc}Z_{sc}} \tag{8}$$

where, p_{sc} is the pressure under normal conditions; M is the relative molecular weight of natural gas; R_g is the molar gas constant; Z_{sc} is the compression factor of natural gas under normal conditions; T_{sc} is the thermodynamic temperature under standard conditions.

The density of natural gas under the condition of gas reservoir is:

$$\rho_g=\frac{pM}{R_g TZ} \tag{9}$$

where, p is the current gas reservoir pressure; T is the gas reservoir temperature; Z is the compression factor of natural gas.

From Eqs. (7)–(9):

$$v=\frac{1}{w_f h}\frac{p_{sc}qTZ}{Z_{sc}T_{sc}p} \tag{10}$$

combining Eq. (10) and Eq. (6):

$$\frac{\mathrm{d}p}{\mathrm{d}x}=\frac{\mu}{k_f w_f h}\frac{p_{sc}qTZ}{T_{sc}Z_{sc}p}+\frac{\beta pM}{w_f^2 h^2 TZ}\left[\frac{p_{sc}qTZ}{T_{sc}Z_{sc}p}\right]^2 \tag{11}$$

integral along the length of compression fracture can be obtained:

$$\frac{p_{wf}^2-p_0^2}{\mu Z}=\frac{2x_f}{k_f w_f h}\frac{p_{sc}qT}{T_{sc}Z_{sc}}+\frac{2x_f\beta MT}{R_g\mu w_f^2 h^2}\left[\frac{p_{sc}q}{T_{sc}Z_{sc}}\right]^2 \tag{12}$$

For homogeneous reservoirs, the pressure of ellipsoid flow can be expressed as:

$$p_i^2-p_{wf}^2=\frac{2p_{sc}\mu qZT}{khT_{sc}x_f}\left(\mathrm{lntanh}\left(\frac{\xi_R}{2}\right)-\mathrm{lntanh}\left(\frac{\pi r_w}{4c}\right)\right) \tag{13}$$

where, p_0 is the bottom hole pressure; p_i is the initial formation pressure of the gas reservoir; p_{wf} is the pressure in the fracture; r_w is the wellbore radius.

Since the pressure of gas at the interface of the two flows is equal, the production of a fracture can be obtained:

$$p_i^2-p_0^2=\frac{2p_{sc}\mu qZT}{khT_{sc}x_f}\left(\mathrm{lntanh}\left(\frac{\xi_R}{2}\right)-\mathrm{lntanh}\left(\frac{\pi r_w}{4c}\right)\right)+\frac{2x_f}{k_f w_f h}\frac{\mu Z p_{sc}qT}{T_{sc}Z_{sc}}+\frac{2x_f Z\beta MT}{R_g w_f^2 h^2}\left[\frac{p_{sc}q}{T_{sc}Z_{sc}}\right]^2 \tag{14}$$

When the production envelope appears to overlap, the production of the repeated area is considered constant (Yu and Sepehrnoori, 2013). As shown in Fig. 3, the production envelope will overlap if the actual well deviates from the planned trajectory. Area shaded in red represent production loss, and its calculation process is as follows.

As shown in the above figure, AQ is an arc segment of the deviation-correction trajectory near fracture W. The fracture P is planned to be fractured on AQ, and fracturing depth is d. The ellipsoid volumes controlled by the fractures is V_t^P and V_t^W respectively, and the overlapping ellipsoid volume is $V_{t,d}^{P,W}$. It is assumed that the daily production of the two fractures is q_t^P and q_t^W respectively. From the perspective of volume flow, the contribution of inter-fracture interference to production is directly proportional to the volume controlled by the influence domain (Yao et al., 2013). Then, at the fracturing depth d, the daily production loss $q_{t,d}^{P,W}$ calculation formula is:

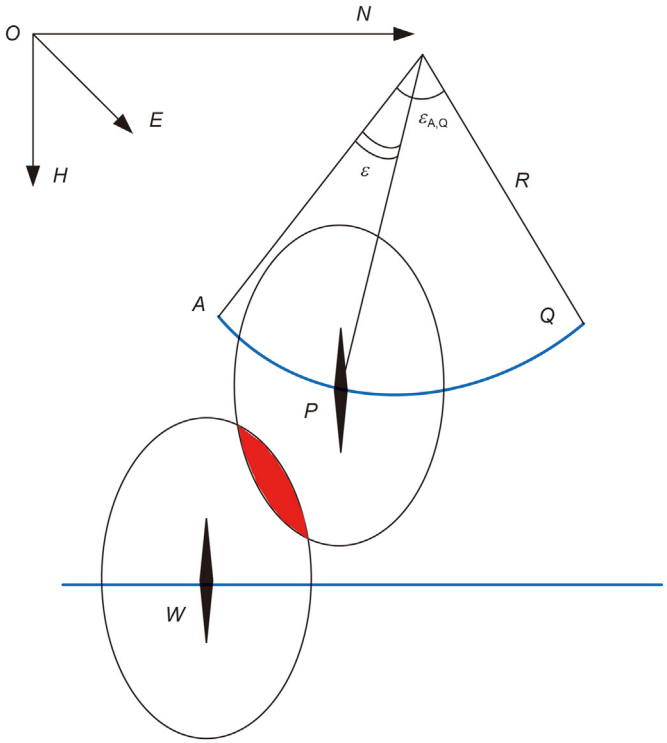

Fig. 3. Schematic diagram of production loss.

$$q_{t,\,d}^{P,\,W} = q_t^P + q_t^W - q_{t,\,d}^P - q_{t,\,d}^W \tag{15}$$

where, $q_{t,\,d}^P$ represents the actual production of fracture P; $q_{t,\,d}^W$ represents the actual production of fracture W.

$$q_{t,\,d}^P = \frac{V_t^P - V_{t,\,d}^{P,\,W}/2}{V_t^P} q_t^P \tag{16}$$

$$q_{t,\,d}^W = \frac{V_t^W - V_{t,\,d}^{P,\,W}/2}{V_t^W} q_t^W \tag{17}$$

$$V_{t,\,\mathrm{d}}^{P,\,W} = f\left(\mathbf{r}_\mathrm{P},\ \mathbf{r}_\mathrm{W},\ \varphi_\mathrm{f},\ V_t^P,\ V_t^W\right) \tag{18}$$

$f(x)$ is the function of calculating the overlapping volume; φ_f is the azimuth angle of fracture; $\mathbf{r}_\mathrm{P}$, $\mathbf{r}_\mathrm{W}$ is the vector diameter of points P and W; $\mathbf{r}_\mathrm{W}$ is $(N_\mathrm{W},\ E_\mathrm{W},\ H_\mathrm{W})$, $\mathbf{r}_\mathrm{P}$ can be expressed as:

$$\begin{cases} N_\mathrm{P} = N_\mathrm{A} + \lambda(\eta \sin\alpha_\mathrm{A} \cos\varphi_\mathrm{A} + \gamma \sin\alpha_\mathrm{Q} \cos\varphi_\mathrm{Q}) \\ E_\mathrm{P} = E_\mathrm{A} + \lambda(\eta \sin\alpha_\mathrm{A} \sin\varphi_\mathrm{A} + \gamma \sin\alpha_\mathrm{Q} \sin\varphi_\mathrm{Q}) \\ H_\mathrm{P} = H_\mathrm{A} + \lambda(\eta \cos\alpha_\mathrm{A} + \gamma \cos\alpha_\mathrm{Q}) \end{cases} \tag{19}$$

where,

$$\begin{cases} \eta = \dfrac{\sin\left(\varepsilon_{\mathrm{A,Q}} - \dfrac{\varepsilon}{2}\right)}{\sin\varepsilon_{\mathrm{A,Q}}} \\ \gamma = \dfrac{\sin\dfrac{\varepsilon}{2}}{\sin\varepsilon_{\mathrm{A,Q}}} \\ \lambda = 2R\sin\dfrac{\varepsilon}{2} \end{cases} \tag{20}$$

N, E and H are the positions of any point in *O-NEH* coordinate system, m; α and φ are well deviation angle and azimuth angle, (°); ε represents the center angle of the arc, (°); R represents the radius of curvature of the arc, m; Subscripts A and Q indicate point A and point Q.

3. Optimization of deviation-correction trajectory

The economics of fracturing depends on the ability to empty the reservoir effectively, and the deviation-correction trajectory should be designed to avoid adjacent wells. The production loss is obtained by analyzing the inter-fracture interference in different fracturing depths. On this basis, a multi-objective optimization model of deviation-correction trajectory is proposed to ensure the feasibility of the trajectory.

3.1. Objective function

Consideration of the need for trajectory control as simple as possible, the design profile of "double-arc" is often adopted for deviation-correction trajectory. The designed trajectory is based on the single arc profile, and then the second arc profile is inclined to reach the planned azimuth and back to the planned trajectory.

When calculating trajectory parameters, some parameters need to be given first, and other parameters can be solved accordingly. In Fig. 4, the straight-line segment OC represents the planned trajectory, and point A is the bottom hole position of the actual well. AC is the designed deviation-correction trajectory. Two fractures W and F are on the adjacent well, and fracture P is located at the fracturing depth d. Suppose that the designed trajectory consists of two inclined arc segments AQ and QC, with curvatures K_1 and K_2 respectively. M is the intersection of the tangent line at points A and Q, N is the intersection of the tangent line at points C and Q. Make $|\mathrm{MQ}| = L_\mathrm{M}$, $|\mathrm{QN}| = L_\mathrm{N}$, $|\mathrm{OC}| = L_\mathrm{OC}$, $A_1 = \mathbf{r}_\mathrm{AO}\cdot\mathbf{t}_\mathrm{A}$, $\cos\theta = \mathbf{t}_\mathrm{A}\cdot\mathbf{t}_\mathrm{C}$. According to the theory of space geometry and vector algebra, the trajectory design equations can be obtained as follows:

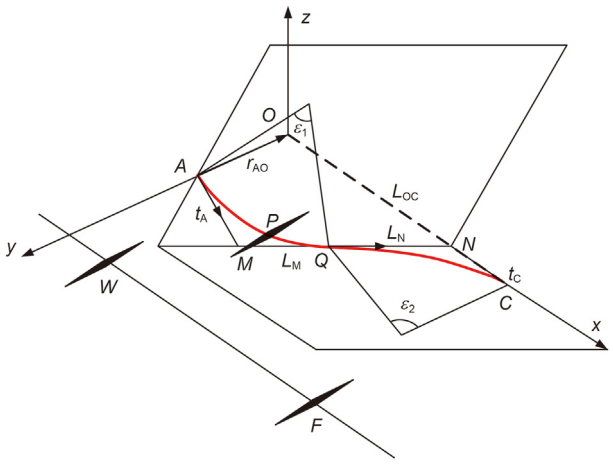

Fig. 4. Schematic diagram of the deviation-correction trajectory.

$$\begin{cases} 2L_\mathrm{N}(L_\mathrm{M}+L_{OC}) - 2(L_\mathrm{M}\cos\theta)(L_\mathrm{N}-L_\mathrm{OC}) + 2A_1L_\mathrm{M} = \mathbf{r}_\mathrm{AO}^2 + L_\mathrm{OC}^2 \\ K_1^2L_\mathrm{M}^2[A_1 + L_\mathrm{N}(1-\cos\theta) + L_\mathrm{OC}\cos\theta] = 2L_\mathrm{M} + L_\mathrm{N}(1+\cos\theta) - L_\mathrm{OC}\cos\theta - A_1 \\ K_2^2L_\mathrm{N}^2[L_\mathrm{M}(1-\cos\theta) + L_\mathrm{OC}] = 2L_\mathrm{N} + L_\mathrm{M}(1+\cos\theta) - L_\mathrm{OC} \end{cases} \tag{21}$$

The trajectory design equations have three equations and five unknowns. The values of the other three parameters can be calculated if the values of any two parameters are given in the parameters L_M, L_N, L_OC, K_1 and K_2 (Wang and Gao, 2016).

In deviation-correction trajectory design, the operator expects the actual well to return to the planned trajectory as soon as possible to reduce production loss economically. When fracture P is on the deviation-correction trajectory, the design trajectory affects the production loss. For the trajectory shown in Fig. 4, the total production loss can be calculated as follows:

$$Q_\mathrm{D} = \sum_1^t \left(q_{t,\,d}^{P,\,W} + q_{t,\,d}^{P,\,F}\right) \tag{22}$$

where, $q_{t,\,d}^{P,\,W}$ and $q_{t,\,d}^{P,\,F}$ are the daily production loss between fracture P and two other fractures respectively, m^3; t is the mining time, day.

In addition to considering production loss, evaluating the trajectory complexity is also essential to optimize trajectory design. As the depth of horizontal wells increases, the trajectory complexity and the drilling risk increases (Liu et al., 2019). Samuel proposed the strain energy of the well profile to quantify the drilling risk of the trajectory (Samuel, 2010). For the designed trajectory shown in Fig. 4, the well profile energy can be calculated as follows:

$$E_\mathrm{W} = K_1^2\Delta L_1 + K_2^2\Delta L_2 \tag{23}$$

where,

$$\Delta L_1 = 2\text{atan}(L_M K_1)/K_1 \tag{24}$$

$$\Delta L_2 = 2\text{atan}(L_N K_2)/K_2 \tag{25}$$

K_1 and K_2 are the curvature of the first arc segment and the second arc segment respectively, rad/m; The unit of L_M and L_N is m.

3.2. Optimization model

Operators prospect to obtain the best deviation-correction trajectory to reduce production loss and drilling risks. Unfortunately, these criteria are often at odds with each other. For example, a smooth trajectory always results in relatively significant production loss. A good trajectory should satisfy all factors and have a minor production loss and a lower well profile energy. Nevertheless, the single-objective optimization method cannot guarantee the best deviation-correction trajectory. Based on this, the objective function of deviation-correction trajectory is:

$$\min F = w_1 f_1^{\text{new}} + w_2 f_2^{\text{new}} \tag{26}$$

where, w_1 and w_2 are the weight of production loss and well profile energy respectively, $0 \le w_i (i = 1,2) \le 1$; f_1^{new} and f_2^{new} are production loss and well profile energy after normalization:

$$f_i^{\text{new}} = \frac{f_i}{f_i^*},\ (i = 1,2) \tag{27}$$

where, f_1 is the optimization result of production loss, f_2 is the optimization result of well profile energy, f_1^* is the optimization result of f_1 when $w_1 = 1$, f_2^* is the optimization result of f_2 when $w_2 = 1$.

In most cases, the curvature of the trajectory, which is not a definite value, can often be determined according to the maximum allowable curvature value (Gu et al., 2020). The length of the designed trajectory must also be within a reasonable range to ensure that the model gives birth to the optimal value. Hence, in multi-objective optimization, the constraint conditions are processed as follows:

$$\begin{cases} x_1^{\min} \le x_1 \le x_1^{\max} \\ x_2^{\min} \le x_2 \le x_2^{\max} \\ x_3^{\min} \le x_3 \le x_3^{\max} \\ x_4^{\min} \le x_4 \le x_4^{\max} \\ x_5^{\min} \le x_5 \le x_5^{\max} \\ x_6^{\min} \le x_6 \le x_6^{\max} \\ g_1(x) = 0 \\ g_2(x) = 0 \\ g_3(x) = 0 \end{cases} \tag{28}$$

$$\begin{cases} g_1(x) = 2x_2(x_1 + x_3) - 2(x_1 \cos\theta)(x_2 - x_3) + 2A_1 x_1 - \mathbf{r}_{AO}^2 - x_3^2 \\ g_2(x) = x_4^2 x_1^2 [A_1 + x_2(1 - \cos\theta) + x_3 \cos\theta] - 2x_1 - x_2(1 + \cos\theta) + x_3 \cos\theta + A_1 \\ g_3(x) = x_5^2 x_2^2 [x_1(1 - \cos\theta) + x_3] - 2x_2 - x_1(1 + \cos\theta) + x_3 \end{cases} \tag{29}$$

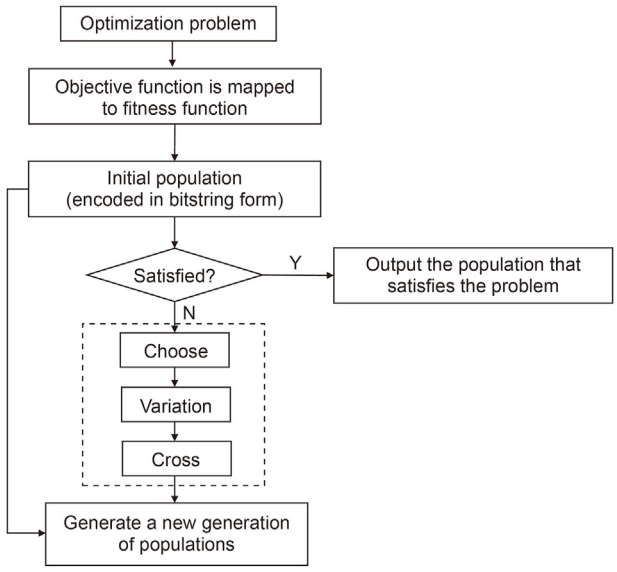

Fig. 5. Flow diagram of GA.

where, x_1, x_2, x_3, x_4, x_5, x_6 represent L_M, L_N, L_{OC}, K_1, K_2, d respectively; $\cos\theta = \mathbf{t}_A \cdot \mathbf{t}_C$, $A_1 = \mathbf{t}_A \cdot \mathbf{r}_{AO}$.

4. Genetic algorithm solution

The optimization design model for the deviation-correction trajectory is a nonlinear optimization problem. Heuristic algorithms, such as genetic algorithm and PSO algorithm, are often used to solve this optimization model. Among them, the genetic algorithm is the most widely used.

Genetic algorithm is a random global search optimization algorithm that simulates the evolution process of biological chromosomes under the rule of survival of the fittest. In this algorithm, individuals obtain better fitness function values through chromosomally encoded selection, crossover and mutation. After repeated iterations, it converges to the optimal value of the function (the most adaptive individual) with the greatest probability. The calculation flow chart of the genetic algorithm is shown in Fig. 5.

5. Case study

5.1. Case 1

The model is applied in Fuling shale gas area in China (Yao et al., 2013), and the main input parameters in the simulation are shown in Table 1.

Due to drilling errors, the actual trajectory often deviates from the planned trajectory by tens of meters. Fig. 6 shows the typical

Table 1
Shale gas reservoir parameters.

Parameters	Value	Units
Horizontal well spacing	250	m
Fracture length	120	m
Wellbore radius	0.05	m
Fracture permeability	30	μm^2
Gas viscosity	0.025	mPa·s
Formation porosity	0.096	1
Comprehensive compressibility of gas	0.12	1/MPa
Gas reservoir thickness	8	m
Permeability of formation	0.00022	μm^2
Formation pressure	27	MPa
Bottom hole pressure	23	MPa
Width of fracture	5	mm
Temperature of formation	80	°C

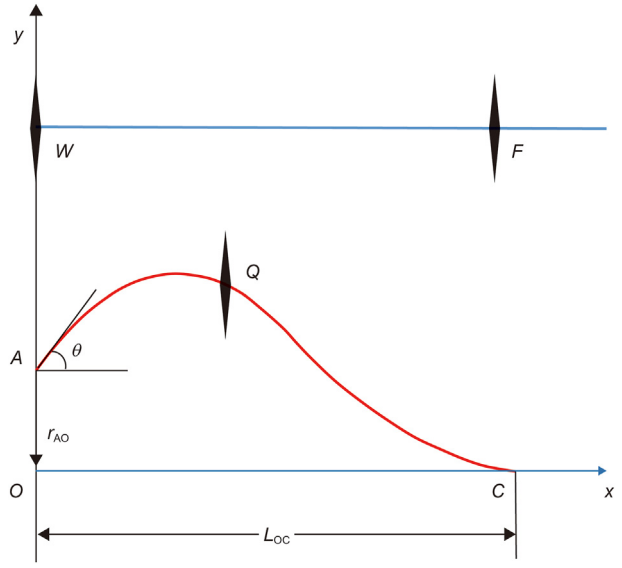

Fig. 6. Typical physical model of fracture located on deviation-correction trajectory.

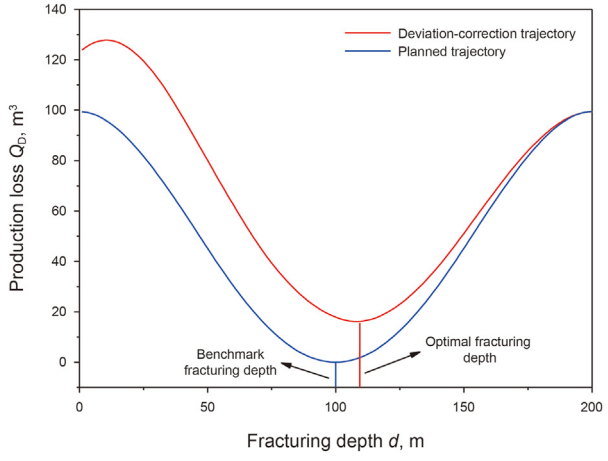

Fig. 7. Production loss varies with fracturing depth.

Table 2
Calculation results of benchmark and optimization on deviation-correction trajectory.

Fracture	d, m	North coordinate, m	East coordinate, m	Q_D, m^3
Benchmark	100	5.9	99.8	18.0
Optimal	108	5.1	107.7	15.9

deviation-correction trajectory of shale gas area. The O point is the origin of the coordinate axis, the xy plane is located on the horizontal plane. The x axis points to the east, and the y axis points to the north. The included angle θ is 9°, and the initial deviation $\mathbf{r}_{AO}$ is 4 m. The coordinates of fracture W and F are (0, 250), (200, 250) respectively, m. Design trajectory parameters: $L_M = L_N = 50.3$ m, $L_{OC} = 200$ m, $K_1 = 4.73°/30$ m, $K_2 = 2.02°/30$ m. Assuming mining time is one year, try to give the optimal fracturing depth.

The production loss at different fracturing depths was simulated to study the influence of the deviation-correction trajectory on production. It can be seen from Fig. 7 that the production loss of the deviation-correction trajectory is greater than the planned trajectory. The planned trajectory had minimal production loss when fracture Q was between two fractures, so the benchmark fracturing depth was 100 m. For the deviation-correction trajectory, the production loss was minimal when the fracturing depth was 108 m. The results show that the deviation-correction trajectory leads to a change in the optimal fracturing depth.

Table 2 shows that when fracturing depth is 100 m, the production loss on the deviation-correction trajectory is 18.0 m^3. When fracturing depth is 108 m, the production loss is 15.9 m^3, down 13.2%. The results show that the proposed model can reduce the production loss of deviation-correction trajectory, and contribute to the efficient development of shale gas.

When the angle θ and deviation $\mathbf{r}_{AO}$ are different, the optimal fracturing depth of different trajectories is as follows (Fig. 8 and Table 3):

5.2. Case 2

When the trajectory parameters are known, the optimization method of fracturing depth has been demonstrated in the previous section. However, in the actual shale gas development, we should also consider the optimal design of deviation-correction trajectory. Based on unknown trajectory parameters, the optimization effect of the model is analyzed. Assuming when the actual well reaches point A, the azimuth of point A is 331°, and the azimuth of planned trajectory is 340°. The well deviation angle of the planned trajectory and point A is 90°. Take point O as coordinate origin, the vector diameters is $\mathbf{r}_W$=(0, 250, 0), $\mathbf{r}_F$=(200, 250, 0), $\mathbf{r}_A$= (0, 19, 0), m. Taking point A as the starting point, the benchmark fracturing depth is 100 m. It is assumed that the maximum curvature allowed for the design trajectory is 11°/30 m, $L_M = L_N$ and the maximum L_{OC} is 200 m (Wang and Gao, 2016). The input value of shale gas reservoir parameters is the same as Case 1, mining time is one year.

In the genetic algorithm parameters, the population size is initially set to 200. The number of iterations is 50, the crossover probability is 0.8, and the mutation probability is 0.1. Taking $w_1 = 0.3$ and $w_2 = 0.7$ as an example, the evolution of the objective function with the iteration steps is shown in Fig. 9.

Three types of trajectories are designed with different weight to return to the planned trajectory from point A. As shown in Table 4 and Fig. 10, if $w_1 = 1$, a trajectory with a minimum production loss of 7.5 m^3 is obtained, and the curvature value takes its upper limit. If $w_2 = 1$, the minimum of the well profile energy is 15.66, and the curvature value takes its lower limit. Assuming that $w_1 = 0.3$ and $w_2 = 0.7$ is the most moderate trajectory, the production loss is 19.5 m^3, and the well profile energy is 17.38. The optimal fracturing depth with different weights is shown in Fig. 11. Generally, the value of two weight factors can be equal to meeting two evaluation criteria simultaneously, and the weight factor can be adjusted according to practical problems.

The curve of gas production changing with time is shown in Fig. 12. In the early stage of production, the gas near the fractures is rapidly displaced into the well, so the initial production is high. As

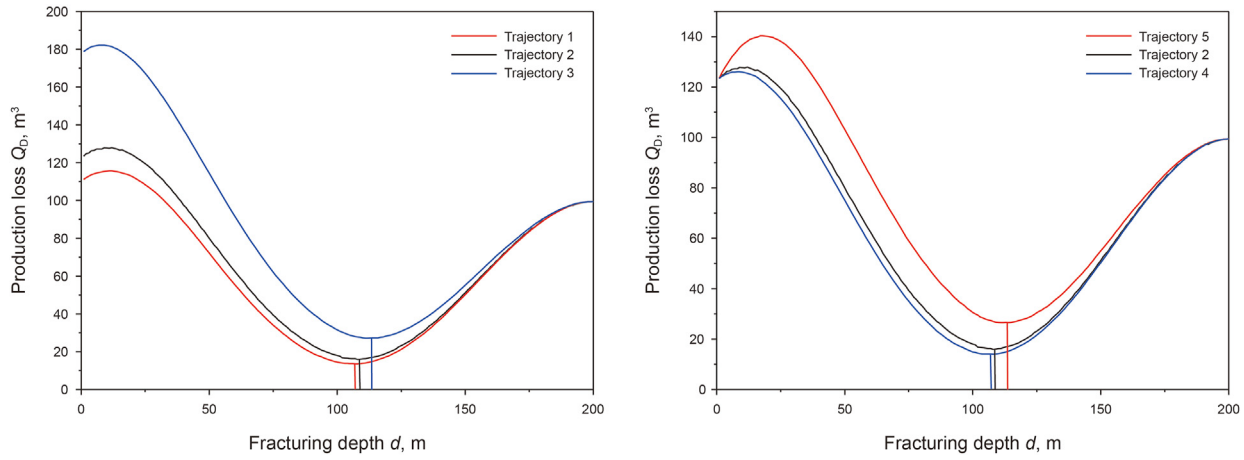

Fig. 8. Variation of fracturing depth and production loss on different trajectories.

Table 3
Optimal fracturing depth and production loss on different trajectories.

Trajectory	r_{AO}, m	θ, °	K_1, °/30 m	K_2, °/30 m	d, m	Q_D, m^3
1	2	9	4.39	1.68	107	13.6
2	4	9	4.73	2.02	108	15.9
3	12	9	6.09	3.37	112	27.1
4	4	6	3.39	1.58	107	14.0
5	4	18	8.75	3.29	112	26.5

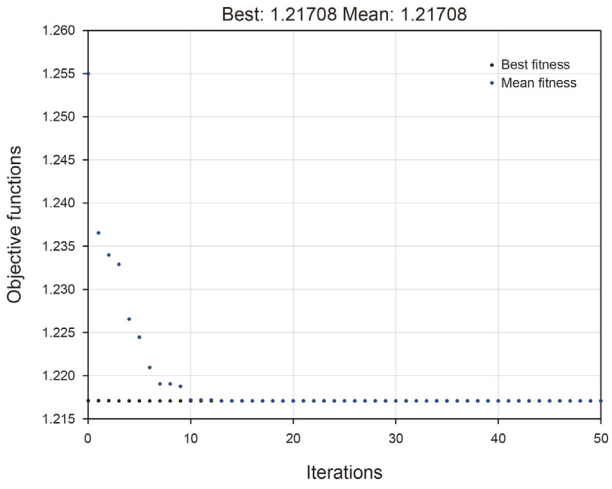

Fig. 9. The change of objective function with the iteration steps when $w_1 = 0.3$, $w_2 = 0.7$.

Table 4
Deviation-correction trajectory parameter table with different weights.

Weight	K_1, °/30 m	K_2, °/30 m	L_{OC}, m	d, m	E_W	Q_D, m^3
$w_1 = 1, w_2 = 0$	11.0	7.4	150	113	28.55	7.5
$w_1 = 0.3, w_2 = 0.7$	7.8	4.9	189	118	17.38	19.5
$w_1 = 0, w_2 = 1$	7.3	4.5	200	120	15.66	23.2

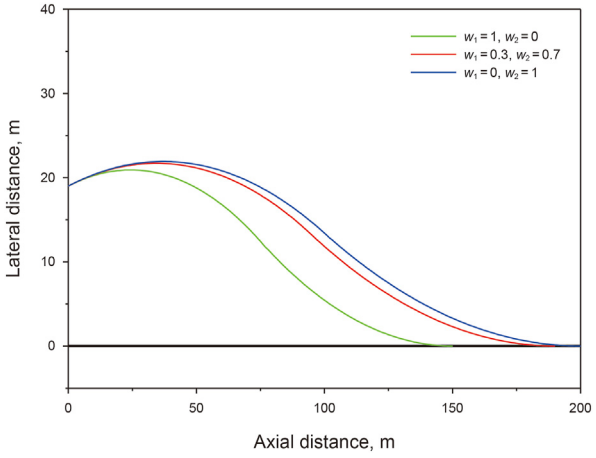

Fig. 10. Deviation-correction trajectory results of different weights.

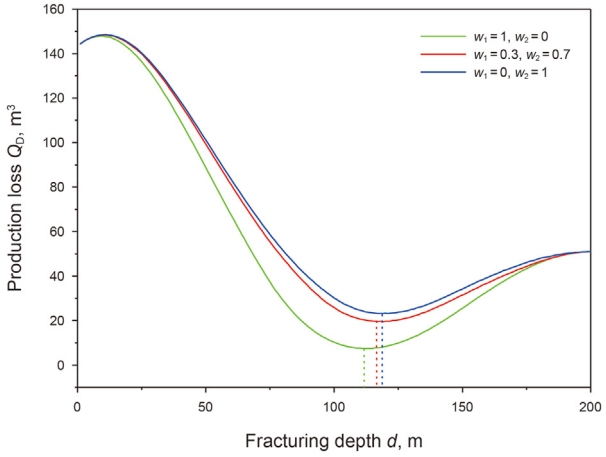

Fig. 11. Fracturing depth results with different weights.

the time increases, the daily production gradually decreases. The inter-fracture interference effect occurred around day 220, and the rate of production decline accelerated further. The rate of reducing production indicates the degree of inter-fracture interference. When $w_1 = 1$, the decline rate of gas production is the slowest. Therefore, if gas production is the main optimization objective, the value of w_1 can be increased to obtain more excellent gas production.

Based on this, the proposed model is compared with the existing model. Under the same production loss, the optimization

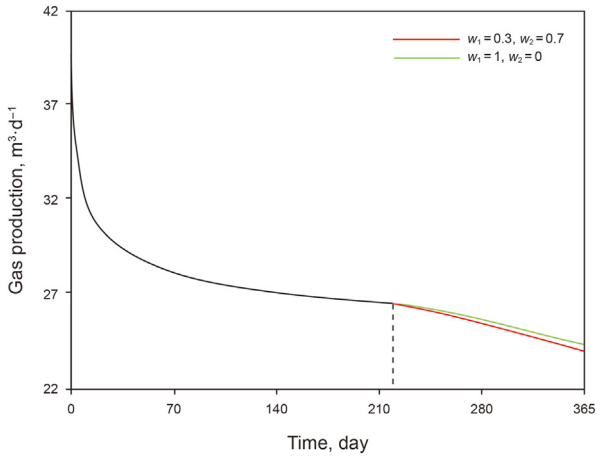

Fig. 12. Influence of deviation-correction trajectory on gas production.

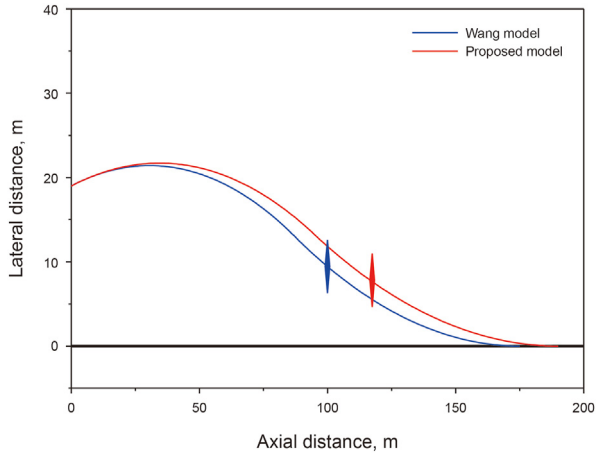

Fig. 13. Comparison diagram of model results.

comparison of trajectory is shown in Fig. 13 and Table 5.

The well profile energy versus well depth is shown in Fig. 14. It can be seen that with the increase of well depth, the well profile energy of proposed model increases more slowly. Therefore, the trajectory dogleg designed by the proposed model has low severity and is not prone to serious problems, such as high torque and resistance. The final well profile energy of proposed model is 17.38, and that of Wang model is 20.6. The results show that proposed model reduces the well profile energy by 15.6%, which can significantly reduce the drilling risk.

The curve of gas production changing with time is shown in Fig. 15. The comparison shows that the proposed model will lead to the inter-fracture interference in advance, but the production declines slower. It should be noted that when the mining time is about 275 days, the proposed model's daily production exceeds that of the Wang model. Although the total production of the two models is the same within one year, the production of the proposed model is higher in the later stage. With the increase of time, the production benefit brought by the proposed model will be more significant.

6. Limitations and discussion

The proposed model aims to guide the optimal trajectory design in the fracturing area. The basic assumption is that the gas reservoir data is known so that input parameters can be selected. However, it should be recognized that actual production loss may be much larger than simulated. If the seepage characteristics of horizontal wells are not considered in practical application, the calculation of production may be inaccurate. In order to simplify the production loss calculation, the following assumptions are made on the factors and conditions considered in the model establishment process :

(1) The upper and lower boundaries of the infinite shale gas reservoir are closed, and the horizontal well is located in the middle of the reservoir.
(2) The fractures opened in the horizontal well section are vertical fractures, and the fracture spacing can be selected arbitrarily.
(3) The reservoir is homogeneous and isotropic, the temperature is constant for unsteady isothermal seepage, and the influence of gravity and capillary force is ignored.

Table 5
Deviation-correction trajectory optimization results for different models.

Model	d, m	Q_D, m^3	K_1, °/30 m	K_2, °/30 m	L_{OC}, m	E_W
Proposed model	118	19.5	7.81	4.94	189	17.38
Wang model	100	19.5	8.8	5.68	175	20.6

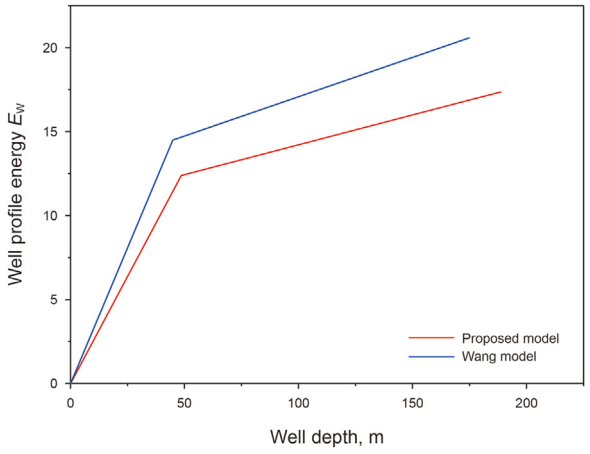

Fig. 14. Well profile energy varies with well depth for different models.

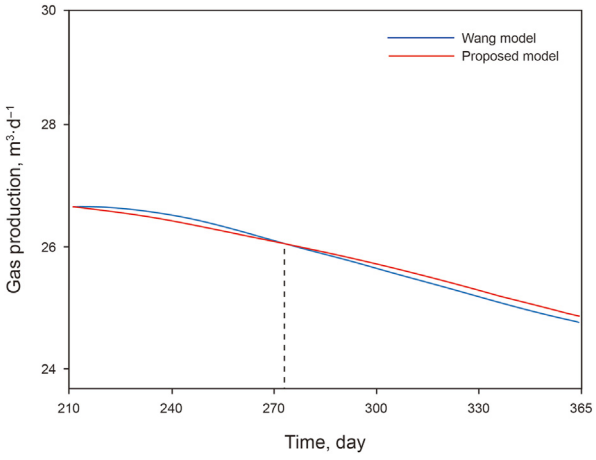

Fig. 15. Gas production varies with time for different models.

(4) The gas flow in the reservoir and fractures is a single-phase flow, and both satisfy Darcy's law.
(5) Gas flows from the reservoir to the fracture and from the fracture to the horizontal well. All production takes place in the fracturing area, regardless of the process of directly flowing from the matrix system to the horizontal well.

7. Conclusions

In shale gas mining, the inter-fracture interference effect is a crucial factor in production loss. Deviation-correction trajectory will significantly influence the inter-fracture interference. The production loss calculation formulas for different fracturing depths are derived, and the multi-objective optimization model of deviation-correction trajectory is established. The results indicate that the production loss is reduced by 13.2% after optimizing the fracturing depth. Besides, the maximum curvature value will result in a trajectory with minimum production loss and maximum well profile energy. Under the same production loss, the proposed model reduces well profile energy by 15.6%. The results show that the proposed model can reduce the probability of drilling accidents and achieve high gas production in the later mining stage. The model could provide theoretical support and guidance for the rapid design of deviation-correction trajectory in fracturing area.

Acknowledgment

The authors gratefully acknowledge the financial support from the Natural Science Foundation of China (No. 42002307), Fundamental Research Funds for the Central Universities (No. 2652019070) and National Key Research and Development Program of China (No. 2018YFC0603405).

References

Bagherian, B., Sarmadivaleh, M., Ghalambor, A., et al., 2010. Optimization of multiple-fractured horizontal tight gas well. In: SPE International Symposium & Exhibiton on Formation Damage Control. https://doi.org/10.2118/127899-MS.
Conlin, J.M., Hale, J.L., Sabathier, J.C., et al., 1990. Multiple-fracture horizontal wells: performance and numerical simulation. In: European Petroleum Conference. https://doi.org/10.2118/20960-MS.
Dou, Z.J., Liu, Y.S., Zhang, J.S., et al., 2022. Optimization of well factory platform mode considering optimal allocation of water resources. Arabian J. Sci. Eng. 47 (9), 11159–11170. https://doi.org/10.1007/s13369-021-05777-3.
Fisher, M.K., et al., 2005. Integrating fracture-mapping technologies to improve stimulations in the Barnett shale. SPE Prod. Facil. 20 (2), 85–93. https://doi.org/10.2118/77441-PA.
Giger, F.M., 1984. Horizontal wells production techniques in heterogeneous reservoirs. In: Society of Petroleum Engineers of AIME, pp. 239–246. https://doi.org/10.2118/13710-MS.
Gu, Y., Gao, D.L., Yang, J., et al., 2020. Optimization design method for the bypass trajectories of infill adjustment wells in the fracturing areas of shale gas fields. Nat. Gas. Ind. 40 (9), 87–96. https://doi.org/10.3787/j.issn.1000-0976.2020.09.011 (in Chinese).
Hanea, R.G., Casanova, P., Hustoft, W., et al., 2017. Well trajectory optimization constrained to structural uncertainties. In: SPE Reservoir Simulation Conference. https://doi.org/10.2118/182680-MS.
Lee, J.W., Park, C., Kang, J.M., et al., Horizontal well design incorporated with interwell interference, drilling location, and trajectory for the recovery optimization. In: SPE/EAGE Reservoir Characterization and Simulation Conference 2009 - Overcoming Modeling Challenges to Optimize Recovery. https://doi.org/10.2118/125539-ms.
Lei, Z.D., Cheng, S.Q., Li, X.F., et al., 2007. A new method for prediction of productivity of fractured horizontal wells based on non-steady flow. J Hydrodynamics Ser. B. 19 (18), 494–500. https://doi.org/10.1016/S1001-6058(07)60145-0.
Liu, Z.C., Samuel, R., 2016. Wellbore-trajectory control by use of minimum well-profile-energy criterion for drilling automation. SPE J. 21 (2), 449–458. https://doi.org/10.2118/170861-PA.
Liu, X.S., Shi, Z., 2002. A new method of path-correction planning with the desired direction. Acta Pet. Sin. 23 (2), 72–76. https://doi.org/10.7623/syxb200202016.
Liu, Y.S., Gao, D.L., Wei, Z., et al., 2019. A new solution to enhance cuttings transport in mining drilling by using pulse jet mill technique. Sci. China Technol. Sci. 62 (5), 875–884. https://doi.org/10.1007/s11431-017-9260-y.
Lu, J., Zhu, T., Tian, D., 2009. Pressure behavior of horizontal wells in dual-porosity, dual-permeability naturally fractured reservoirs. In: SPE Middle East Oil and Gas Show and Conference. https://doi.org/10.2118/120103-MS.
Lyu, Z.H., Lei, Q.H., Yang, L., et al., 2021. A novel approach to optimising well trajectory in heterogeneous reservoirs based on the fast-marching method. J. Nat. Gas Sci. Eng. 88, 103853. https://doi.org/10.1016/j.jngse.2021.103853.
Magalhaes, F., Zhu, D., Amini, S., et al., 2007. Optimization of fractured-well performance of horizontal gas wells. In: SPE - 2nd International Oil Conference and Exhibition in Mexico, June 2007. https://doi.org/10.2118/108779-MS.
Maus, S., DeVerse, J.S., 2016. Simulation of recovery losses due to positional errors in wellbore placement. In: SPE/AAPG/SEG Unconventional Resources Technology Conference. https://doi.org/10.15530/URTEC-2016-2458814.
Ozkan, E., Brown, M., Raghavan, R., et al., 2011. Comparison of fractured-horizontal-well performance in tight sand and shale reservoirs. SPE Reservoir Eval. Eng. 14 (2), 248–259. https://doi.org/10.2118/121290-PA.
Samuel, R., 2010. A new well-path design using clothoid spiral (curvature bridging) for ultra-extended-reach drilling. SPE Drill. Complet. 25 (3), 363–371. https://doi.org/10.2118/119459-PA.
Shandrygin, A., 2019. Optimization of unconventional gas reservoirs development by horizontal wells with multiple hydraulic fracturing. In: SPE Russian Petroleum Technology Conference 2019. https://doi.org/10.2118/196741-MS.
Soliman, M.Y., Hunt, J.L., Azari, M., 1996. Fracturing horizontal wells in gas reservoirs. In: SPE Eastern Regional Conference and Exhibition. https://doi.org/10.2118/59096-PA.
Wang, Z.Y., Gao, D.L., 2016. Multi-objective optimization design and control of deviation-correction trajectory with undetermined target. J. Nat. Gas Sci. Eng. 33, 305–314. https://doi.org/10.1016/j.jngse.2016.05.028.
Yao, T.Y., Zhu, W., Li, J., et al., 2013. Fracture mutual interference and fracture propagation roles in production of horizontal gas wells in fractured reservoir. J. Cent. South Univ. (Science Technology) 44 (4), 1487–1492 (in Chinese).
Yu, W., Sepehrnoori, K., 2013. Optimization of multiple hydraulically fractured horizontal wells in unconventional gas reservoirs. J. Petrol. Technol. 476–491. https://doi.org/10.2118/164509-ms.